



Immobilization of P450 BM-3 monooxygenase on mesoporous molecular sieves with different pore diameters

Evelyne Weber^a, Demet Sirim^a, Tino Schreiber^{b,1}, Bejoy Thomas^b, Jürgen Pleiss^a, Michael Hunger^b, Roger Gläser^c, Vlada B. Urlacher^{a,*}

^a Institute of Technical Biochemistry, Universitaet of Stuttgart, Allmandring 31, 70569 Stuttgart, Germany

^b Institute of Chemical Technology, Universitaet of Stuttgart, Pfaffenwaldring 55, 70569 Stuttgart, Germany

^c Institute of Chemical Technology, University of Leipzig, Linnéstraße 3, 04103 Leipzig, Germany

ARTICLE INFO

Article history:

Received 9 October 2009

Received in revised form 22 January 2010

Accepted 22 January 2010

Available online 1 February 2010

Keywords:

P450 BM-3

Mesoporous molecular sieves

SBA-15

MCM-41

Immobilization

ABSTRACT

The immobilization of the isolated heme domain of P450 BM-3 (BM3H.F87A) on two mesoporous molecular sieves, MCM-41 (pore diameter 25 Å) and SBA-15 (pore diameter 60 Å and 133 Å) was examined systematically, and the activity of the immobilized enzyme toward *para*-nitrophenoxydodecanoic acid (12-*p*NCA) and *n*-octane was determined. Hydrogen peroxide was utilized as source of electrons and oxygen to support the monooxygenase activity of BM3H.F87A. The mesoporous materials were characterized by X-ray diffraction and nitrogen adsorption analyses before and after immobilization. The results revealed that the immobilization efficiency of MCM-41 and SBA-15 after single immersion was strongly affected by the pH value of the enzyme solution, initial enzyme concentration and agitation conditions. By modelling the 3D structure *in silico* and performing electrostatic potential calculations, the pH-dependence of the enzyme immobilization could be explained and a possible orientation of the protein on mesoporous materials was predicted. The oxidizing activity of the immobilized enzyme was found to depend on pore diameter and accessibility of the substrate for the enzyme. The highest activity toward 12-*p*NCA of 830 nmol product/mg P450/min was observed with BM3H.F87A immobilized on SBA-15 with pore diameter 133 Å. Enzyme activity toward *n*-octane was similar for the enzyme immobilized on SBA-15 of 60 Å and 133 Å, and was at least two-fold higher as compared to a system with free enzyme.

© 2010 Elsevier B.V. All rights reserved.

1. Introduction

In general, immobilization with respect to enzyme stabilization refers to associating an enzyme with an insoluble matrix, so that it can be reused under stabilized conditions. Immobilized biocatalysts offer several other advantages, like improved enzyme storage and operational stability, resistance to elevated temperatures and organic (co)-solvents, the possibility for continuous processes and greater control over enzymatic reactions. Although immobilization to solid carriers is perhaps the most frequently used strategy to improve the stability of enzymes, only a few reports of successful cytochrome P450 immobilization can be found in literature. Cytochrome P450 enzymes (P450s) are heme containing proteins that catalyze oxygenation of a vast variety of organic molecules. One of the problems regarding the use and immobiliza-

tion of P450 enzymes is their dependency on the pyridine co-factors NADH and NADPH and the need for the corresponding reductases, which transfer electrons from NAD(P)H to the heme group. The first example on immobilization of P450s dates back to 1988 when Wiseman and co-workers [1] immobilized purified P450s from *Saccharomyces cerevisiae* along with the corresponding reductase by entrapment in calcium alginate or in polyacrylamide, or by adsorption on cyanogen bromide-activated sepharose. A decade later, the plant CYP71B1, fused to a P450 reductase, was immobilized onto colloidal liquid aphrons [2]. Kelly and co-workers reported the co-immobilization of prokaryotic CYP105D1 with a ferredoxin onto the ionic exchange resin DE52-72 [3]. However, most of these systems suffered from the leaching of the enzyme activity from the support.

Previously we have reported the immobilization of the P450 BM-3 from *Bacillus megaterium* (CYP102A1) and some of its mutants on different supports [4]. P450 BM-3 monooxygenase is a self-sufficient natural fusion flavocytochrome (119 kDa) consisting of a heme domain and a diflavin reductase domain [5]. The enzyme was unable to adsorb neither on celite, a porous silicate matrix derived from diatomaceous soil, nor on Eupergit C via covalent

* Corresponding author.

E-mail address: Vlada.Urlacher@itb.uni-stuttgart.de (V.B. Urlacher).

¹ Institute for Interfacial Engineering, Universitaet of Stuttgart, Nobelstr. 12, 70569 Stuttgart, Germany.

binding. Negative results obtained with polypropylene derivatives and phenyl-, octyl- and butylsepharose showed that procedures based on hydrophobic interactions were also unsuitable for the efficient immobilization of P450 BM-3. P450 BM-3 binds to anion exchangers such as DEAE and SuperQ [4]. However, the most substrates and products of the oxidation reaction also adsorbed on these matrices. In addition, enzyme leaching from the carrier occurs in buffers with high ionic strength. Furthermore, the purified P450 BM-3 A74G/F87V/L188Q mutant was successfully encapsulated in a sol–gel matrix derived from tetraethoxyorthosilicate (TEOS) upon polymerization. The entrapment of P450 BM-3 in this sol–gel-type material resulted in a very high long-term storage stability of the enzyme at different temperatures. A half-life of 29 days was measured at 25 °C for immobilized P450 BM-3 and only 2 days for the free enzyme. A sol–gel immobilized P450 BM-3 mutant was able to oxidize substrates of diverse substance classes such as terpenoids, polyaromatic hydrocarbons, *n*-alkanes, and fatty acid analogs with high activity [4]. However, since the entrapment of P450 BM-3 was performed during polymerization of TEOS, we were not able to control pore diameter and pore geometry properly. The use of ordered mesoporous silicates, synthesized using surfactant templating routes and therefore having defined pore diameter and pore geometry, would clarify these aspects. Since the first report by Diaz and Balkus in 1996 [6] various commercially available enzymes such as cytochrome *c* [7], lysozyme [8], lipase [9,10] and albumin [11] have successfully been immobilized on ordered mesoporous materials like MCM-41, MCM-48 (Mobil Composition of Matter) SBA-15 or SBA-16 (Santa Barbara). In some cases proteins were adsorbed only on the external surface area of mesoporous materials, in the others – immobilized within their pores. In the meantime only two reports dedicated to P450 monooxygenases were published [12,13]. Both reports describe immobilization of rabbit CYP2C9 and human CYP2B4 on aluminum-substituted MCM-41 containing aluminum ions at different ratios. Interestingly, catalytic activity of immobilized CYP2C9 and CYP2B4 was observed even in the absence of the cytochrome P450 reductase, which is necessary for electron transfer from NADPH to the heme group. The authors suggested that electron transfer to the immobilized P450s can occur through the Lewis acid, i.e., the Al-centers in the silicate walls [12].

In the present study the immobilization of the isolated heme domain of P450 BM-3 (without the reductase domain) on two mesoporous ordered materials, MCM-41 (pore diameter 25 Å) and SBA-15 (pore diameter 60 Å and 133 Å), was systematically examined. For comparison, a commercial silica gel with a broad pore diameter distribution was included into this study, too. The aim of this study was to develop an effective immobilization procedure and to investigate the effect of the pore diameter on the loading capacity of both materials and oxygenase activity of the immobilized P450 BM-3 heme domain.

2. Experimental

2.1. Materials

All chemicals reagents were of analytical grade purity and purchased from Roth (Karlsruhe, Germany) and Fluka (Steinheim, Germany). H₂O₂ was purchased as a 30 wt.% solution from Fluka. The stock solution was prepared freshly in 50 mM potassium phosphate buffer, pH 7.5. Silica gel-Type 62 and sodium water glass (25.5–28.5 wt.% SiO₂, 7.5–8.5 wt.% Na₂O, rest: water) were obtained from Merck (Germany). 12-*para*-nitrophenoxydodecanoic acid (12-*p*NCA) was synthesized as described elsewhere [14] and dissolved in dimethyl sulfoxide (DMSO).

2.2. Preparation and mutagenesis of the P450 BM-3 heme domain

In our previous work the gene CYP102A1 encoding the cytochrome P450 BM-3 has been amplified from genomic DNA of *B. megaterium* ATCC 14581 and cloned into the pET28a(+)-vector yielding the pET-28a.BM-3 construct [15]. The gene fragment coding for the P450 BM-3 heme domain was amplified from pET-28a.BM-3 using the following primers: 5′-3′: GCGGATCCATGACAATTAAGAAATGCCTCAGC; 5′-3′: GCGAATTCT-TAGCGTACTTTTTAGCAGACTGTTC. The primer for the 3′-end of the gene contains an additional stop codon. The amplified gene as well as the pET28a(+)-vector were cut using the endonucleases *Bam*HI and *Eco*RI and then ligated together by T4-DNA ligase. The replacement of the phenylalanine at position 87 by smaller alanine was performed using the Quick-Change Kit (Stratagene). The primers were as follows: 5′-3′: gcaggagacgggttagctacaagctggacgc and 5′-3′: gcgtccagctttagctaacccgtctctcgc. PCR was carried out following the manufacturer's protocol. The correct gene insertion and mutation were checked by sequencing. The His6-tagged P450 BM-3 F87A heme domain (further referred to as BM3H.F87A) was expressed in *Escherichia coli* BL21(DE3) and purified on Ni-NTA sepharose as described previously for the holoprotein [4]. The P450 concentrations were quantified from the CO-binding difference spectra of the reduced form as described elsewhere [16]. The extinction coefficient of 91 mM⁻¹ cm⁻¹ was used for calculations.

2.3. Immobilization of the P450 F87A heme domain on mesoporous materials

If not stated otherwise 1.5 mL of purified BM3H.F87A with a final concentration of 15–150 μM was added to 20 mg of a mesoporous material. The immobilization procedure was optimized upon different agitation conditions such as stirring, slow rotation at 15 rpm or intensive mixing. Experiments with stirring were carried out with a magnetic stirrer in a covered beaker. Experiments with rotation were carried out in a Rotamix (RM-1, ELMI, Latvia). Intensive mixing was performed in a Beadmill (MM2000, Retsch, Haan, Germany). Immobilization was performed during 1–24 h at 10 °C. The solids with the immobilized enzyme were recovered by centrifugation (10 min, 2000 g, 4 °C). The supernatant was used for estimation of the concentration of non-immobilized active P450 by measuring CO-difference spectra. The recovered solid fractions were washed four times with 50 mM potassium phosphate buffer, pH 7.5, and were stored then at –20 °C before use. CO-difference spectra measured with washing solutions were used for estimation of enzyme leaching. For sequential immersion the already one or more time loaded portion of a mesoporous material was reloaded again under equal conditions. The recovered solid was washed four times with 50 mM potassium phosphate buffer, pH 7.5 between reloading steps.

2.4. Activity toward *p*-nitrophenoxydodecanoic acid (12-*p*NCA)

P450 BM-3 activity assays were performed using the *p*NCA assay [14]. The reaction was carried out at room temperature in a final volume of 1.0 mL containing 50 mM potassium phosphate buffer, pH 8.1, 200 μM 12-*p*NCA dissolved in DMSO (final concentration 1%), and the corresponding amount of the purified enzyme. The reaction was started by adding 10 mM H₂O₂. Formation of *p*-nitrophenolate was followed at 410 nm on an Ultraspec 3000 photometer (Pharmacia Biotech, Uppsala, Sweden) and calculated using extinction coefficient of 13.2 mM⁻¹ cm⁻¹. Activity measurements with immobilized BM3H.F87A (20 mg for each experiment) were carried out under stirring in a flow-through cuvette at room temperature. Formation of *p*-nitrophenolate was followed with a Nicolet evolution 1000 photometer (Thermo Electron Corpo-

ration). All activity measurements were carried out at least in triplicate.

For the identification of enzyme leaching under process conditions the reaction mixture (without the loaded materials) was taken from the flow-through cuvette after 3 and 5 min of the reaction, and used for measuring CO-difference spectra and activity of the enzyme toward lauric acid. The pNCA test could not be applied here because the solution was already yellow. The reaction with lauric acid was monitored by GC–MS as described elsewhere [17].

2.5. Conversion of *n*-octane with immobilized P450 F87A heme domain

To maintain the equal P450 concentration in all experiments, the respective amount of immobilized BM3H.F87A was suspended in 1 mL 50 mM KPi pH 7.5, supplemented with 20 μ L of a 10 mM *n*-octane solution in ethanol and 10 mM H₂O₂. After 2 h the reaction mixture was centrifuged, and the supernatant was extracted twice with 300 μ L dichloromethane. The combined organic layers were supplemented with internal standard 1-decanol, dried over magnesium sulphate and concentrated to a volume of 100 μ L. Reaction products and unreacted substrate were measured on GC/MS (Shimadzu, Japan) using a FS-Supreme-5 column and identified by MS. The temperature gradients were as follows: (1) 40 °C for 1 min, (2) 40–67 °C at 2 °C/min, (3) 67–75 °C at 1 °C/min, (4) 75–280 °C at 30 °C/min. Pure samples of the substrate and potential reaction products 2-, 3-, and 4-octanols were available. Equal amounts of these substances dissolved in dichloromethane were applied to the column. From the resulting GC/MS trace the ratio of the peak areas corresponding to the substrates and products were calculated. These ratios were used to determine the molar ratios of substrates and products emerging from the biotransformations. Therefore equal dichloromethane–water partition coefficients for educts and products were assumed.

2.6. Synthesis of ordered mesoporous materials

2.6.1. MCM-41

MCM-41 was synthesized according to a modified procedure reported in literature [18]. Briefly, 8.13 g sodium water glass was added to 120 g demineralized water and stirred for 30 min. A second solution was prepared by dissolving 4.48 g tetradecyltrimethylammonium bromide in 30 g demineralized water, addition of 10 g ethanol and stirring for 30 min. The two solutions were combined under stirring to obtain a clear gel. After additional stirring for 30 min, 15.0 g 4N H₂SO₄ were added slowly and stirring was continued for 1 h. The resulting gel was transferred into Teflon-lined stainless steel autoclaves and kept at 150 °C for 20 h. After cooling, the solid product was separated by filtration, washed thoroughly with hot water (80 °C) and ethanol and, then, calcined at 550 °C first in a nitrogen atmosphere for 12 h and, subsequently, in air for 6 h.

2.6.2. SBA-15 (60 Å)

For the synthesis of SBA-15, a procedure reported by Choi et al. [19] was followed. Accordingly, 6.92 g of the tri-block copolymer (poly(ethylene oxide)-poly(propylene oxide)-poly(ethylene oxide)) P123 was dissolved in 43.2 g demineralized water and 8.75 g concentrated aqueous hydrochloric acid. Another solution was prepared by diluting 25.9 g sodium water glass with 69.5 g demineralized water and dissolving 0.27 g NaOH. This solution was added to the acidic tri-block copolymer solution at 35 °C under stirring. Stirring was continued for 24 h and, thereafter, the gel was placed in a Teflon-lined autoclave which was heated for 24 h at 100 °C. The solid product was separated, washed and calcined as described for MCM-41 above.

2.6.3. SBA-15 (133 Å)

Large pore SBA-15 was synthesized according to Vinu and co-workers [20]. Typically, 4 g of the tri-block copolymer poly(ethylene glycol)-*block*-poly(propylene glycol)-*block*-poly(ethylene glycol) (EO₂₀PO₇₀EO₂₀) was dispersed in 30 g of water and 120 g of 2 M HCl solution and stirred for 5 h at room temperature. Subsequently, 9.5 g of tetraethyl orthosilicate (TEOS) was added drop-wise to the homogeneous solution at room temperature under constant stirring. The resulting gel was aged at 40 °C for 24 h and finally heated at 150 °C for 48 h. The solid was separated by filtration and dried at 80 °C overnight. Calcination was performed by heating the obtained powder material in air at 200 °C and 400 °C for 3 h at both temperatures and with the heating rate of 1 °C/min. Finally the temperature was increased to 550 °C and kept for 12 h in air to fully decompose the tri-block copolymer.

2.7. Characterization of mesoporous materials

Powder X-ray diffraction (XRD) patterns of the ordered mesoporous materials were collected on a Siemens D 5000 instrument using CuK α radiation (30 mA, 40 kV). The step width and time amounted to 0.02° and 3 s, respectively.

The textural properties of the samples, i.e., the specific BET surface areas, BJH pore volumes and pore size distributions were calculated from the nitrogen adsorption isotherms recorded at –196 °C using a Micromeritics ASAP 2010 equipment. Before the sorption measurements, the solid samples were pre-treated at 300 °C for unloaded samples and at 40 °C for samples loaded with enzyme under vacuum (<10^{–2} mbar) for 12 h.

2.8. Modelling P450 BM-3 heme domain and MD simulation

To obtain a homology model of the P450 BM-3 heme domain, two crystal structures were used as templates: the P450 BM-3 heme domain and a fusion protein between heme domain and FMN-domain [21,22]. The template structures were obtained from the Protein Data Bank (PDB entries 1BU7 and 1BVY). The N-terminal His6 tag, the C-terminal loop from residue 456 to 472, and the mutation F87A were modelled using MODELLER [23].

The initial model structure was refined by energy minimization, and a molecular dynamics (MD) simulation [24] of 600 ps was performed using the SANDER module of the AMBER 9 program suite [25]. The all-atom force field ff99 [26] was used, including the heme force field modification [27]. Prior to the simulation, the system was minimized using the steepest descent algorithm for 500 steps and then switching to the conjugate gradient algorithm for 1500 steps. The MD simulation was performed in implicit solvent by applying the generalized Born solvation model [28]. In the equilibration phase of 20 ps, a restraint force of 0.1 kcal/Å² mol was applied to the main chain atoms and a time step of 1 fs, a constant temperature of 300 K, and a cut-off value of 12 Å were used. After the equilibration, a MD simulation of 600 ps was performed with a time step of 2 fs and a maximum cut-off of 999 Å to ensure that it is larger than the protein size. To preserve the backbone structure a restraint force of 0.1 kcal/Å² mol was applied to main chain atoms of residues 36–493. For constraining the bond length involving hydrogen atoms the SHAKE algorithm [29] was applied with the default tolerance of 0.00001 Å and bond interactions involving hydrogen atoms were omitted.

For the visualization of the structures and the trajectories, Visual Molecular Dynamics (VMD) [30] and PyMOL [31] were used. To determine the molecular size of the protein, the minimal and maximal coordinates of the structure were calculated and a bounding box was constructed. The width of the bounding box corresponds to the maximum diameter of the protein.

2.9. Calculation of the titration curve and the electrostatic potential

For the calculation of the titration curve and the electrostatic potential, the complete sequence of BM3H.F87A was considered. The titration curve of the protein including the heme was calculated by MCCE [25,32] with a dielectric constant of the protein and the solvent of 8 and 80, respectively. Electrostatics was calculated by DELPHI using the finite Poisson–Boltzmann procedure [30] as implemented in the MCCE method. PARSE atomic charges and radii were used [27]. To visualize the charge distribution of P450 BM-3, the electrostatic potential was mapped on the structure using PyMOL.

3. Results and discussion

3.1. Characterization of the support materials

P450 BM-3 hydroxylates long-chain fatty acids in the presence of molecular oxygen and the cofactor NADPH. Various mutants of P450 BM-3 were shown to accept a broad range of substrates [33–37]. The heme domain of P450 BM-3 was found to catalyze the same reactions as the holoenzyme in the presence of hydrogen peroxide instead of dioxygen and the costly cofactor NADPH by following the so-called “peroxide shunt” [34,36]. As reported by Li and co-workers the replacement of phenylalanine at position 87 by alanine offered a higher peroxygenase activity of the BM-3 heme domain compared to the wild type enzyme [36]. The heme domain of P450 BM-3 F87A (further referred to as BM3H.F87A) was constructed as described in Section 2 and immobilized on three different silicates. The physical properties of the solid supports have a large influence on immobilization. Specific surface area, average pore diameter, and total specific pore volume were calculated from nitrogen adsorption isotherms and are collected in Table 1. Silica gel (Type 62) has unordered pores of non-uniform diameter ranging from 20 to 250 Å (mean pore diameter: 114 Å) and a specific surface area of ca. 327 m²/g. This material was used in order to realize the effect of the structure and pore diameter of enzyme loading capacity.

MCM-41 and SBA-15 are two commonly used ordered mesoporous molecular sieves which are characterized by channels of uniform dimension arranged in a strictly regular, parallel, non intersecting hexagonal manner [38,39]. Generally, SBA-15 possesses pores with an adjustable uniform diameter between 60 Å and 150 Å, whereas MCM-41 typically has a pore diameter of approximately 20–60 Å. Besides that, SBA-15 has thick hydrothermal stable silica walls, different from MCM-41 which has thinner walls. The MCM-41 material used in this study has a pore diameter of 25 Å and a specific surface area of 1290 m²/g; SBA-15 was prepared with two differently large pore diameters of 60 Å and 133 Å with the corresponding specific surface areas of 828 and 380 m²/g. All three materials exhibit the well known type IV adsorption isotherms (Brunauer definition). As expected, no sorption hysteresis was observed for MCM-41, while a pronounced sorption hysteresis was found for the two SBA-15 materials. The sorption isotherms for the two SBA-15 materials before and after loading with enzyme are

Table 1
Physicochemical properties of the mesoporous materials used in this study.

Material	Pore diameter (Å)	BET surface area (m ² /g)	Total pore volume (cm ³ g ⁻¹)
MCM-41	25	1290	0.99
SBA-15	60	828	0.92
SBA-15	133	380	1.26
Silica gel	20–250	327	1.27

shown in Figs. 3 and 5 and will be discussed later. Moreover, the XRD-patterns show the characteristic reflections for ordered mesoporous materials with hexagonally arranged pores. Results of XRD characterization of the samples will also be discussed below.

3.2. Optimization of the immobilization procedure

The first set of experiments was conducted under various conditions in order to optimize the immobilization procedure. 20 mg of a mesoporous material were added to a P450 solution with initial concentration of 32 μM, mixed together and incubated as outlined below. The P450 loading at any particular time was calculated by centrifuging the solid material and measuring the P450 concentration of the supernatant, and taking these values from the initial P450 concentration, respectively.

The stability experiments with BM3H.F87A under the experimental conditions chosen for the immobilization processes revealed no loss in enzyme activity or solubility under stirring or slow rotation at different pH values and 10 °C or room temperature within 24 h. However, activity was completely lost upon intensive mixing in a bead mill already after 1 h. Therefore, mixing in a bead mill was excluded from the following experiments.

We observed, that agitation conditions influenced enzyme loading on both MCM-41 and SBA-15 (60 Å). Independently on immobilization time, pH and initial P450 concentration, a loading capacity of only 7–14 mg/g could be achieved after stirring. Under slow rotation the enzyme loading increased up to 30–34 mg/g for SBA-15 with a pore diameter of 60 Å and up to 22–26 mg/g for MCM-41 (25 Å), when immobilization was performed from a solution volume of 1.5 mL. For further experiments slow rotation was chosen as the most appropriated method. Our experiments demonstrated that under rotation in 1.5 mL volume equilibrium between enzyme solution and the solid materials as assessed from a constant loading was achieved already after 2 h.

The effect of pH on enzyme loading capacity was investigated using buffered enzyme solutions with different pH values ranging from pH 6.0 to pH 8.0 (supplementary Fig. 1). The highest enzyme loading after a single immersion of 33 mg P450 per 1 g SBA-15 (60 Å), 27 mg P450 per 1 g MCM-41 and 10 mg P450 per 1 g silica gel was observed at pH 7.0 (Fig. 1).

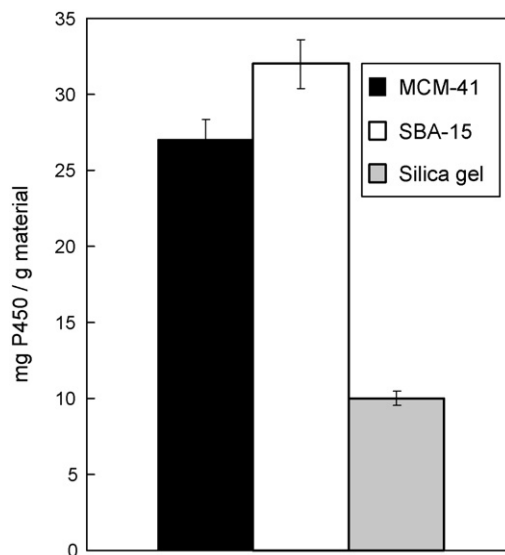
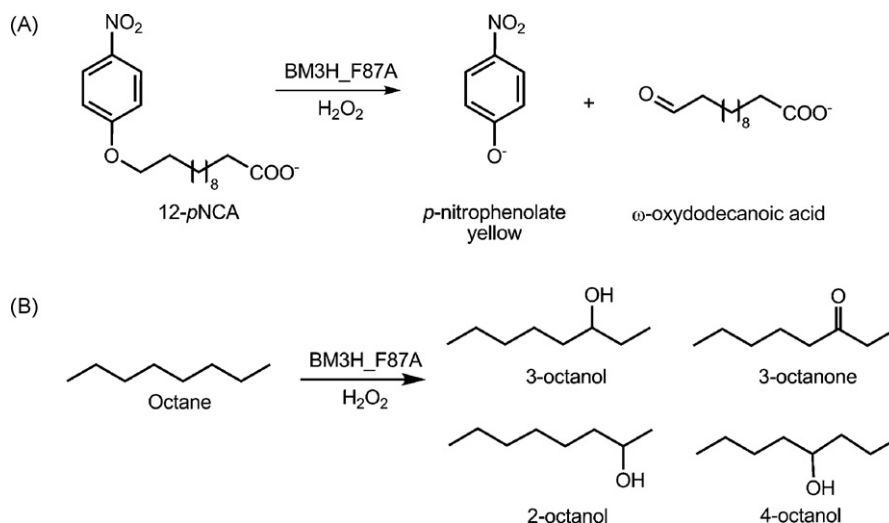


Fig. 1. Immobilization of BM3H.F87A on MCM-41 (25 Å), SBA-15 (60 Å) and silica gel after a single immersion at pH 7.0; enzyme concentration 35 μM, volume 1.5 mL.



Scheme 1. Hydroxylation of (A) 12-pNCA to *para*-nitrophenolate and (B) of *n*-octane to a mixture of secondary alcohols catalyzed by BM3H.F87A.

3.3. Influence of pore diameter on enzyme loading and activity

The dimensions of BM3H.F87A were estimated based on the crystal structure (PDB entries 1BU7 and 1BVY) after addition of the linker region and His6- tag in an extended conformation. During a 600 ps MD simulation their conformation changed to a more compact structure. The size of the modelled protein is $80 \times 70 \times 60 \text{ \AA}$, slightly larger than the crystal structure without the linker and His6- tag ($70 \times 60 \times 60 \text{ \AA}$). The distance along the minor axis (60 \AA) is similar to the pore diameter of SBA-15 (60 \AA), while the major axis exceeds the pore diameter by 20 nm. Thus, it is expected that the protein is able to bind inside the pores of silica gel and SBA-15, but not MCM-41 [12].

The preliminary experiments described above demonstrated the effect of pore diameter on enzyme loading capacity. We suggest that the low immobilization capacity of silica gel of $<10 \text{ mg/g}$ (measured after washing) relates to a broad distribution of pore diameters with an average at 114 \AA , which is significantly larger than the diameter of the enzyme. In this case up to 60% of P450 activity was removed from the support during washing as the enzyme molecules are probably only loosely adsorbed onto the internal surface of the silica gel. Almost no changes in the N_2 -adsorption isotherms or pore size distribution curves before and after loading BM3H.F87A on silica gel were observed (see supplementary Fig. 2).

The enzyme loading on ordered MCM-41 with a pore diameter of 25 \AA after a single immersion measured after repeating washing (15–20% P450 lost) was higher than that of sol-gel (27 mg/g vs. 10 mg/g). For an activity test, oxidation of *p*-nitrophenoxydodecanoic acid (12-pNCA) was chosen as a model reaction, because it allows the simple photometrical measurement of *p*-nitrophenolate which is produced during the reaction (Scheme 1A). The specific activity of the enzyme of $11 \text{ nmol product/mg P450/min}$ was very low compared to $1100 \text{ nmol product/mg P450/min}$ measured with the free enzyme. According to the literature data most proteins of molecular mass higher than 40 kDa cannot enter the pores of MCM-41 with pore diameters in the range of $20\text{--}30 \text{ \AA}$ and are only adsorbed on the external surface [6]. If enzyme is only immobilized on the external surface, the observed specific activity is usually low and enzyme leaching occurs. Our results with BM3H.F87A as well as physico-chemical analyses by N_2 -adsorption confirmed this observation. After loading of MCM-41 with the enzyme, no pore volume could be detected any more. However, the absence of any reflections in the X-ray diffractogram (Fig. 2A) indicates, that the long-range order of the MCM-41 was lost. To test whether the loss of the nitrogen sorption capacity is due to a pore blocking, the enzyme-loaded MCM-41 was re-calcined at $540 \text{ }^\circ\text{C}$ in air, but neither the XRD pattern typical for MCM-41-materials nor the nitrogen sorption capacity were restored. We therefore conclude that the loss of nitrogen sorption

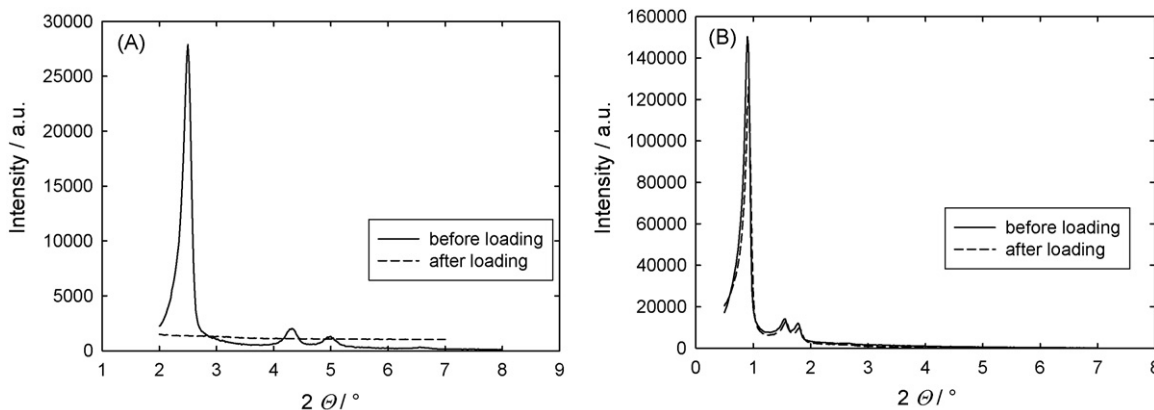


Fig. 2. XRD powder patterns of the mesoporous sieves before and after enzyme immobilization at pH 7.0: (A) MCM-41 (25 \AA); (B) SBA-15 (60 \AA).

Table 2
Loading capacity of the mesoporous materials and specific activity of immobilized BM3H.F87A toward 12-pNCA.

BM3H.F87A	Loading capacity (mg P450/g material)	Specific activity (nmol product/mg P450/min)	Immobilization procedure
Free enzyme	–	1100 ± 33	–
MCM-41 (25 Å)	27 ± 3	11 ± 2	Single immersion
SBA-15 (60 Å)	32 ± 4	112 ± 8	Single immersion
SBA-15 (60 Å)	50 ± 3	130 ± 10	Sequential immersing
SBA-15 (133 Å)	90 ± 6	830 ± 28	Single immersion

capacity could be due to a partial or total collapse of the ordered mesopore system in MCM-41 while loading with the enzyme. Note that the long-range order of SBA-15 (60 Å) remains intact even after loading of this support with the enzyme (Fig. 2B). This finding can be explained by the higher wall thickness of SBA-15 compared to MCM-41, and the resulting higher stability of SBA-15 toward the enzyme-containing solution during the immobilization steps.

Several reports suggest that for higher activity and stability the protein of interest should be immobilized inside the pores. However, the question whether the pore diameter should be significantly larger than the protein to allow for diffusion of protein and substrate into the pore or if pore and protein should be of similar size to increase stability and protection of the protein is under discussion, which is reflected by very contradictory reports published in this respect [40]. Takahashi et al. investigated immobilization of the horseradish peroxidase and reported that for its enhanced activity and stability in organic solvents, pores for the immobilization should match the size of the protein, because, if the pore will be too big, the enzyme will not be well protected [41,42]. Our investigations demonstrated that although the immobilization capacity of SBA-15 (60 Å) was similar to MCM-41 (25 Å) (25–32 mg/g) after a single immersion, the observed specific activity of the immobilized enzyme toward 12-pNCA was at least 10-fold higher (11 nmol product/mg P450/min vs. 112 nmol product/mg P450/min) (Table 2). This is a first hint for the accommodation of BM3H.F87A molecules inside the pores of SBA-15. Our results demonstrate that by matching pore size with protein size higher enzyme activity can be attained. However, since almost the same amount of P450 was immobilized on SBA-15 (60 Å) and MCM-41 (25 Å) under the same conditions, the loading is obviously further influenced by the available pore volume and surface area.

Another indication of adsorption of the enzyme within the pores of SBA-15 comes from the comparison of the nitrogen sorption isotherms of this material before and after loading with enzyme and that of the amorphous silica gel. In SBA-15 (60 Å), the specific surface area was reduced from 828 m²/g before to 539 m²/g after loading with enzyme (Fig. 3). At variance, the specific surface area was reduced from 327 to only 302 m²/g for silica gel. Evi-

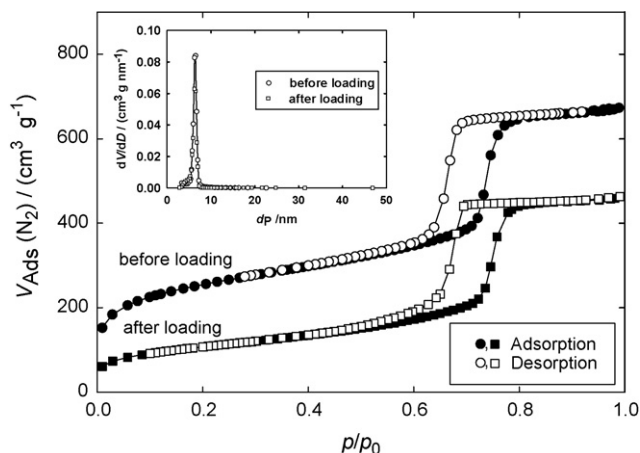


Fig. 3. Changes of N₂-adsorption isotherms ($T = -196^\circ\text{C}$) and pore size distribution curves from the adsorption (●, ■) and desorption (○, □) before (○) and after (□) loading BM3H.F87A on SBA-15 (60 Å).

dently, a lower amount of enzyme was adsorbed on silica gel, where only surface area within rather large pores is available and enzyme removal during washing is facilitated. An at least partial immobilization of the enzyme within the pores of SBA-15 is therefore likely. Also note that the lower closure point of the hysteresis loop for the SBA-15 after enzyme immobilization (Fig. 3) is shifted to a relative pressure <0.6 which might be interpreted in terms of unevenly shaped pores due to presence of enzyme on the inner surface.

3.4. Optimization of enzyme loading onto SBA-15

In an attempt to improve immobilization onto SBA-15 (60 Å), we increased the initial P450 concentration in solution. Generally, after a simple immersion in a total volume of 1.5 mL, the loading capacity of SBA-15 increased only until a BM3H.F87A-concentration of 20 μM (Fig. 4A). Further increase up to 50 μM P450 did not change loading capacity of SBA-15 (60 Å). Furthermore, P450 concentrations higher than 50 μM limited somehow the immobilization process, resulting even in reduced loading capacity. 25 mg were loaded on 1 g SBA-15 when 31 μM BM3H.F87A was used, only 17 mg/g with 75 μM, and enzyme concentration of 112 μM led to the lowest enzyme loading of 10 mg/g. The calculation of the inner pore volume (Table 1) suggested that in all cases it was high enough for immobilization of at least a 50-fold higher P450 concentration. According to the modelling studies it is expected that the protein is able to bind inside the pores of SBA-15 (60 Å). However, the observed behaviour indicates the existence of some sort of diffusion hindrance or pore blockage which prevents the protein molecules from diffusing into the inner particle region. Remarkably, this hindrance could be overcome by sequen-

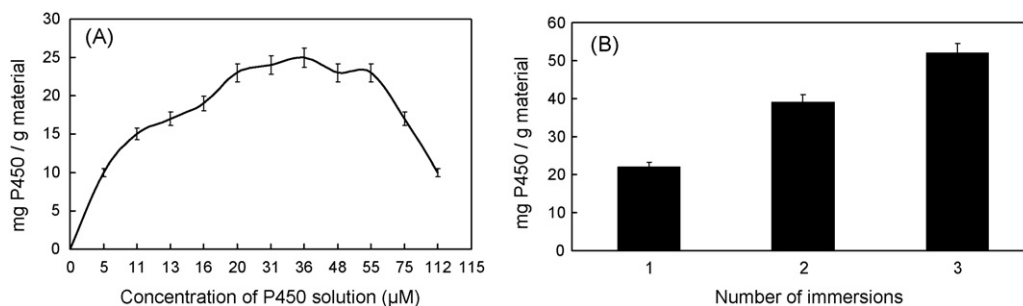


Fig. 4. Optimization of enzyme loading onto SBA-15; (A): Dependence of the immobilization efficiency of SBA-15 (60 Å) on initial enzyme concentration; (B) Sequential immersion of SBA-15 (60 Å) at enzyme concentration of 36.4 μM.

tial immersing the same portion of supporting material with fresh enzyme solution. 20 mg SBA-15 was loaded with a 36.4 μM P450 solution several times in 1.5 mL under equal conditions (Fig. 4B). After the first round of immobilization 22 mg/g was loaded onto SBA-15. More than 90% of P450 was immobilized from the loading solution. After several washing steps the same material was loaded again, which led to an increased loading capacity up to 37 mg/g. Only 68% of the enzyme was adsorbed during this second immersion round. The next immersion resulted in totally 50 mg/g, however only 35% of P450 was immobilized in this case. Nevertheless, also in this case the specific activity of BM3H.F87A retained on the similar level and achieved 130 nmol/mg P450/min (Table 2).

The fact that reloading with fresh enzyme solutions increased the amount of the absorbed protein, and that high concentrations of the initial P450 solution resulted in a lower immobilization efficiency indicated, that loading might be kinetically controlled. Our further experiments demonstrated that increase of immobilization volume from 1.5 up to 10 mL represents an alternative way for improving the loading capacity of SBA-15 at P450 concentrations of $>50 \mu\text{M}$ or higher. In 3 mL of 48 μM BM3H.F87A an almost three-fold increase in loading capacity (75 mg/g) was achieved. When the same experiment was performed in 10 mL, loading capacity reached 180 mg/g within 2 h (data not shown). These results confirmed the presence of diffusion hindrance or pore blockage which prevents the protein molecules from diffusing into the inner particle region.

The N_2 -adsorption isotherms estimated before and after immobilization of BM3H.F87A onto SBA-15 (60 Å) demonstrated a reduction of pore volume from 828 to 539 m^2/g (see above). However, as discussed earlier, such a finding does not necessarily give absolute evidence for entrance of the enzyme into the pores, as pore blockages at the entrance to the mesopores can reduce pore volumes and surface areas even when the protein molecules have not fully entered the pore [43–45]. Furthermore, since the specific activity of BM3H.F87A immobilized on SBA-15 with a pore diameter of 60 Å was still lower compared to its free, i.e., unsupported form, we tested SBA-15 with a pore diameter of 133 Å. This diameter is twice as large as the longest axis of BM3H.F87A and should be enough for “in-pore” protein accommodation. As expected, the loading capacity of SBA-15 (133 Å) was higher and reached 50 mg/g when the experiment was carried out in 1.5 mL of 26.8 μM P450 solution. Moreover, no P450 was removed during the washing steps. In 10 mL of 16.2 μM P450 solution 90 mg active enzyme could be immobilized onto 1 g SBA-15 and increased up to 210 mg/g SBA-15 after two additional immersions. For identification of enzyme leaching under reaction conditions the reaction mixture (without the loaded materials) was analysed after 3 and 5 min of p-NCA oxidation as described in Section 2. Neither spectral data no activity measurements indicated the presence of the P450 monooxygenase in the reaction mixture within the first 5 min of reaction.

Upon loading with enzyme, the specific surface area of the SBA-15 (133 Å) decreased from 380 to 268 m^2/g . Although this decrease is less pronounced than that for the SBA-15 with the smaller pore diameter of 60 Å, it is still remarkable. Moreover, in the case of SBA-15 (133 Å) a significant change of the pore diameter distribution was observed (Fig. 5). While the pore size distribution was generally broadened, the most apparent effect is that a larger amount of smaller pore diameters than in the enzyme-free support material is observed. Also, the maximum of the pore size distribution was shifted from 133 to 117 Å. Taken together, the reduction in specific surface area and the shift of the pore size distribution to significantly lower values can be considered as evidence for an immobilization of BM3H.F87A within the mesopores of SBA-15 (133 Å).

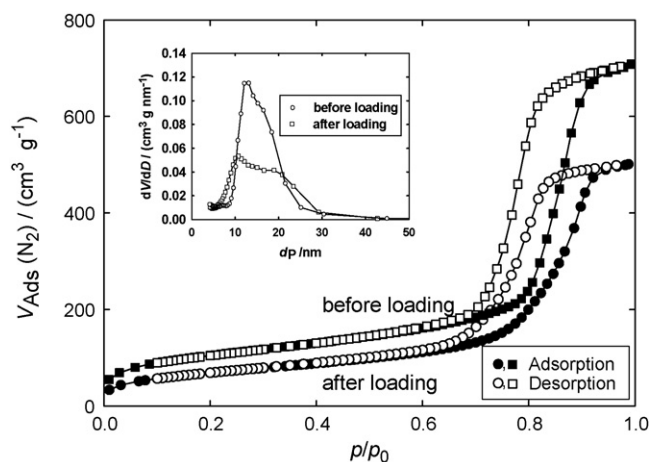


Fig. 5. Changes of N_2 -adsorption isotherms ($T = -196^\circ\text{C}$) and pore size distribution curves from the adsorption (●, ■) and desorption (○, □) before (○) and after (□) loading BM3H.F87A on SBA-15 (133 Å).

Additionally, the specific activity of the immobilized BM3H.F87A as measured with 12-pNCA was tested. For the enzyme supported on SBA-15 (133 Å) it increased up to 840 nmol product/mg P450/min (Table 2). As mentioned in the introduction, previously we immobilized a triple P450 BM-3 mutant in a sol-gel matrix derived from tetraethoxyorthosilicate. In that study the natural holoenzyme, consisting of a monooxygenase domain fused to a reductase domain was used. As electron donor the cofactor NADPH, supported by regeneration with formate dehydrogenase was applied. Under these conditions the specific activity of the immobilized enzyme toward 12-pNCA reached 884 nmol/mg P450/min (in the original manuscript expressed as 0.89 U/mg P450). This value is comparable with activity obtained with the enzyme immobilized on SBA-15 (133 Å). One should take into account that the molecular mass of the holoenzyme is two-fold higher than that of the separated monooxygenase.

Nevertheless, the obtained value was still lower compared to the free enzyme (1100 nmol/mg P450/min). As possible reasons for this difference in specific activity (1) a non-optimal orientation of enzyme molecule in the mesopores of the support, and (2) insufficient accessibility of the substrate 12-pNCA for immobilized BM3H.F87A, can be considered.

3.5. Modelling the P450 BM-3 heme domain

To explain the observed results and to elucidate enzyme orientation on SBA-15, the electrostatic properties of the protein and the immobilization matrix were considered. It was assumed that long-range electrostatic interactions are dominating the pH-dependent interactions. Because the pore size exceeds the diameter of the protein, the matrix was modelled as a planar surface. Thus, a titration curve of BM3H.F87A was calculated for pH values between 3 and 10. The total charge of the protein was decreasing from 32 to -18 with increasing pH, with a pI of 5.4. The electrostatic potential was calculated for pH 6.0, 7.0, and 8.0 (Fig. 6). At pH 7.0 where the maximal amount of BM3H.F87A was immobilized, the protein is negatively charged (total charge of -7.9). The electrostatic surface of BM3H.F87A consists of large patches of negative charge with a small patch of positive charge proximal to the heme group (Fig. 6). At this pH, the surface of the matrix is negatively charged, since the point-of-zero of aluminium silica is approximately at pH of 3.0 [46]. Previously, it has been shown that charged proteins bind preferably to a surface with the opposite charge, less well to a surface with the same charge, and least to an uncharged surface [47]. It has been suggested that binding occurs via charged surface patches,

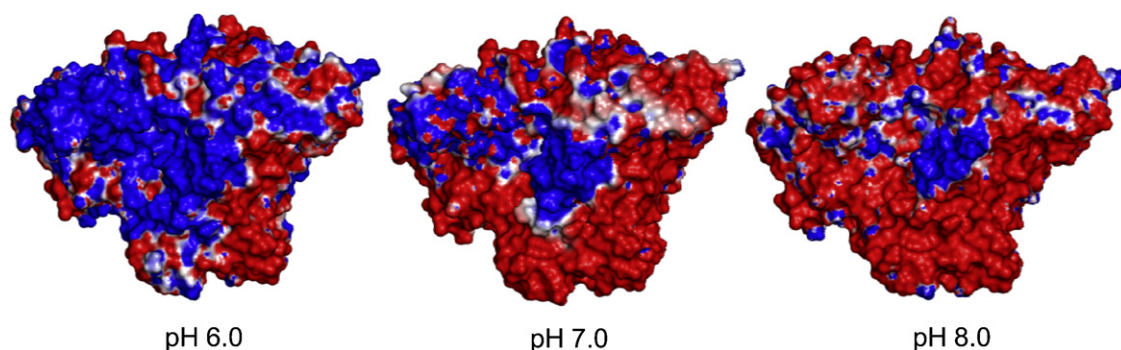


Fig. 6. Electrostatic potential at pH 6.0, 7.0 and 8.0 mapped on the surface of the structure model of P450 BM-3 heme domain. A positive surface potential is shown in blue and a negative surface potential is shown in red.

thus the orientation of a protein binding to a positively or a negatively charged surface is expected to change [47]. This observation could explain the peak in the immobilization efficiency at pH 7.0. At this pH, the matrix is slightly charged, and the positive patch of P450 is large enough to enable binding, despite of the repulsion between the negatively charged surface and the negative charge of the protein. At a higher pH value, however, the negative charge of the protein and the surface increase, and the size of the positive patch of the protein decreases, which leads to a decrease of immobilization efficiency. For pH values below 7.0, the charge at the surface decreases, which leads to a decrease of immobilization efficiency, as the surface becomes neutral. In addition, at pH 7.0 the protein binds in the favourable orientation, since the positive patch is located proximal to the heme at the reductase binding site, opposite to the entrance to the substrate binding site. This suggest that substrate binding pocket of the enzyme should be accessible for substrates at least in SBA-15 with pore diameter of 133 Å, and so cannot be a limiting factor for specific activity.

3.6. Activity and stability of immobilized BM3H.F87A toward *n*-octane

In our previous work we observed that the substrate 12-*p*NCA as well as its oxidation products can bind to negatively charged supporting materials like DEAD-cellulose. In order to elucidate whether either *p*NCA or the *p*-nitrophenolate bind to SBA-15 and this can affect the activity of the immobilized P450, hydrophobic *n*-octane was used as substrate. The measurements with purified free BM3H.F87A as well as with immobilized enzyme were carried out for 2 h under continuous shaking at room temperature.

Conversion of *n*-octane reached 18–20% with immobilized BM3H.F87A and was even higher than in the system with free enzyme (9%). As reaction products the regioisomers 2-, 3-, 4-octanol and 3-octanone were identified in molar ratio of approx 2: 4: 3: 1 (Scheme 1B). These values correlate to those reported previously [33] and indicate that the regioselectivity of BM3H.F87A was not changed upon immobilization.

Generally the observed total P450 activity for both immobilized and free enzyme was quite low and reached 35–60 nmol total product/mg P450 (Table 3). As *n*-octane oxidation by BM3H.F87A

Table 3

Conversion of *n*-octane by free and immobilized BM3H.F87A after 2 h. Identical amounts of free and immobilized enzyme (3 mg) and 10 μM H₂O₂ were used in all experiments.

Enzyme	Substrate conversion (%)	Activity (nmol total product/mg P450)
Free enzyme	9	30 ± 4
SBA-15 (60 Å)	20	62 ± 6
SBA-15 (133 Å)	18	59 ± 7

is much slower than the oxidation of 12-*p*NCA, the enzyme stability in the presence of 10 mM H₂O₂ becomes a limiting factor for conversion. Judging from the obtained conversion values we suggest, that the enzyme hidden inside the pores stayed stable over at least two-times longer period of time and produced more oxidized products than free enzyme under the same conditions. Since conversion values for SBA-15 with different pore diameters were similar, obviously *n*-octane can reach the immobilized P450 even inside the smaller pores. This may indicate that lower activity of BM3H.F87A immobilized onto SBA-15 (133 Å) toward 12-*p*NCA compared to its free form might be due to insufficient accessibility of the substrate 12-*p*NCA for the enzyme. However, deactivation of the enzyme inside the pores cannot be excluded completely, since this parameter cannot be elucidated.

4. Conclusions

Efficient immobilization of P450 monooxygenases can only be achieved when a detailed understanding of the enzyme properties is combined with a tailoring design of mesoporous supports. Our results on the immobilization of the heme domain BM3H.F87A on mesoporous molecular sieves MCM-41 (25 Å) and SBA-15 (60 Å and 133 Å) demonstrated the importance of a match between pore diameter and protein dimensions. The enzymatic activity was retained only after immobilization of BM3H.F87A inside the pores of SBA-15. If the enzyme was absorbed on the external surface of the material as in the case of MCM-41, its activity was very low. Furthermore, for the “in pore” immobilized BM3H.F87A the nature of the substrate plays a critical role. Reduced accessibility of 12-*p*NCA for the immobilized BM3H.F87A is probably a limiting factor, which leads to reduction in enzyme activity. For *n*-octane, the operational stability of the enzyme becomes a more essential issue, reflecting the fact that the immobilized enzyme showed higher activity than its free form.

Acknowledgements

This work was financially supported by the Deutsche Forschungsgemeinschaft (SFB 706), the Ministerium für Wissenschaft, Forschung und Kunst des Landes Baden-Württemberg and the Fonds der Chemischen Industrie. We acknowledge valuable contributions by Alexander Steudle.

Appendix A. Supplementary data

Supplementary data associated with this article can be found, in the online version, at doi:10.1016/j.molcatb.2010.01.020.

References

- [1] D.L. King, M.R. Azari, A. Wiseman, *Methods Enzymol.* 137 (1988) 675–686.
- [2] S.B. Lamb, D.C. Lamb, S.L. Kelly, D.C. Stuckey, *FEBS Lett.* 431 (1998) 343–346.
- [3] M. Taylor, D.C. Lamb, R.J. Cannell, M.J. Dawson, S.L. Kelly, *Biochem. Biophys. Res. Commun.* 279 (2000) 708–711.
- [4] S. Maurer, V. Urlacher, H. Schulze, R.D. Schmid, *Adv. Synth. Catal.* 345 (2003) 802–810.
- [5] H. Li, T.L. Poulos, *Nat. Struct. Biol.* 4 (1997) 140–146.
- [6] J.F. Diaz, K.J. Balkus, *J. Mol. Catal. B: Enzym.* 2 (1996) 115–126.
- [7] C.H. Lee, J. Lang, C.W. Yen, P.C. Shih, T.S. Lin, C.Y. Mou, *J. Phys. Chem. B* 109 (2005) 12277–12286.
- [8] A. Katiyar, S. Yadav, P.G. Smirmiotis, N.G. Pinto, *J. Chromatogr. A* 1122 (2006) 13–20.
- [9] E.L. Pires, E.A. Miranda, G.P. Valenca, *Appl. Biochem. Biotechnol.* 98 (2002) 963–976.
- [10] A. Salis, D. Meloni, S. Ligas, M.F. Casula, M. Monduzzi, V. Solinas, E. Dumitriu, *Langmuir* 21 (2005) 5511–5516.
- [11] S.W. Song, K. Hidajat, S. Kawi, *Langmuir* 21 (2005) 9568–9575.
- [12] M.C.R. Hernandez, J.E.M. Wejebe, J.I.V. Alcantara, R.M. Ruvalcaba, L.A.G. Serrano, J.T. Ferrara, *Microporous Mesoporous Mater.* 80 (2005) 25–31.
- [13] M. Rosales-Hernandez, L. Kispert, E. Torres-Ramirez, D. Ramirez-Rosales, R. Zamorano-Ulloa, J. Trujillo-Ferrara, *Biotechnol. Lett.* 29 (2007) 919–924.
- [14] U. Schwaneberg, C. Schmidt-Dannert, J. Schmitt, R.D. Schmid, *Anal. Biochem.* 269 (1999) 359–366.
- [15] S. Pflug, S.M. Richter, V.B. Urlacher, *J. Biotechnol.* 129 (2007) 481–488.
- [16] T. Omura, R.J. Sato, *J. Biol. Chem.* 239 (1964) 2370–2378.
- [17] S.C. Maurer, K. Kuehnel, L.A. Kaysser, S. Eiben, R.D. Schmid, V.B. Urlacher, *Adv. Synth. Catal.* 347 (2005) 1090–1098.
- [18] T. Boger, R. Roesky, R. Glaser, S. Ernst, G. Eigenberger, J. Weitkamp, *Microporous Mater.* 8 (1997) 79–91.
- [19] M. Choi, W. Heo, F. Kleitz, R. Ryoo, *Chem. Commun. (Camb)* (2003) 1340–1341.
- [20] A. Vinu, V. Murugesan, O. Tangermann, M. Hartmann, *Chem. Mater.* 16 (2004) 3056–3065.
- [21] I.F. Sevioukova, H.Y. Li, H. Zhang, J.A. Peterson, T.L. Poulos, *Proc. Natl. Acad. Sci. U.S.A.* 96 (1999) 1863–1868.
- [22] H.M. Berman, T. Battistuz, T.N. Bhat, W.F. Bluhm, P.E. Bourne, K. Burkhardt, Z. Feng, G.L. Gilliland, L. Iype, S. Jain, P. Fagan, J. Marvin, D. Padilla, V. Ravichandran, B. Schneider, N. Thanki, H. Weissig, J.D. Westbrook, C. Zardecki, *Acta Crystallogr. D. Biol. Crystallogr.* 58 (2002) 899–907.
- [23] A. Sali, T.L. Blundell, *J. Mol. Biol.* 234 (1993) 779–815.
- [24] K.K. Khan, S. Mazumdar, S. Modi, M. Sutcliffe, G.C. Roberts, S. Mitra, *Eur. J. Biochem.* 244 (1997) 361–370.
- [25] R.E. Georgescu, E.G. Alexov, M.R. Gunner, *Biophys. J.* 83 (2002) 1731–1748.
- [26] J.M. Wang, P. Cieplak, P.A. Kollman, *J. Comput. Chem.* 21 (2000) 1049–1074.
- [27] D. Sitkoff, K.A. Sharp, B. Honig, *J. Phys. Chem. B* 98 (1994) 1978–1988.
- [28] C.J. Cramer, D.G. Truhlar, *Chem. Rev.* 99 (1999) 2161–2200.
- [29] R.C. Walker, M.F. Crowley, D.A. Case, *J. Comput. Chem.* 29 (2008) 1019–1031.
- [30] P.A. Zoretic, H. Fang, A.A. Ribeiro, *J. Org. Chem.* 63 (1998) 7213–7217.
- [31] W.L. Delano, in: San Carlos, CA, USA: DeLano Scientific, 2002.
- [32] E.G. Alexov, M.R. Gunner, *Biophys. J.* 72 (1997) 2075–2093.
- [33] D. Appel, R.D. Schmid, C.A. Dragan, M. Bureik, V.B. Urlacher, *Anal. Bioanal. Chem.* 383 (2005) 182–186.
- [34] P.C. Cirino, F.H. Arnold, *Angew. Chem. Int. Ed. Engl.* 42 (2003) 3299–3301.
- [35] M. Landwehr, L. Hochrein, C.R. Otey, A. Kasrayan, J.E. Backvall, F.H. Arnold, *J. Am. Chem. Soc.* 128 (2006) 6058–6059.
- [36] Q.S. Li, J. Ogawa, S. Shimizu, *Biochem. Biophys. Res. Commun.* 280 (2001) 1258–1261.
- [37] V.B. Urlacher, A. Makhsumkhanov, R.D. Schmid, *Appl. Microbiol. Biotechnol.* 70 (2006) 53–59.
- [38] C.T. Kresge, M.E. Leonowicz, W.J. Roth, J.C. Vartuli, J.S. Beck, *Nature* 359 (1992) 710–712.
- [39] M. Kruk, M. Jaroniec, C.H. Ko, R. Ryoo, *Chem. Mater.* 12 (2000) 1961–1968.
- [40] S. Hudson, J. Cooney, E. Magner, *Angew. Chem. Int. Ed. Engl.* 47 (2008) 8582–8594.
- [41] H. Takahashi, B. Li, T. Sasaki, C. Miyazaki, T. Kajino, S. Inagaki, *Chem. Mater.* 12 (2000) 3301–3305.
- [42] H. Takahashi, B. Li, T. Sasaki, C. Miyazaki, T. Kajino, S. Inagaki, *Microporous Mesoporous Mater.* 44 (2001) 755–762.
- [43] J. Deere, E. Magner, J.G. Wall, B.K. Hodnett, *J. Phys. Chem. B* 106 (2002) 7340–7347.
- [44] A. Vinu, V. Murugesan, M. Hartmann, *J. Phys. Chem. B* 108 (2004) 7323–7330.
- [45] A. Vinu, C. Streb, V. Murugesan, M. Hartmann, *J. Phys. Chem. B* 107 (2003) 8297–8299.
- [46] A.J. O'Connor, A. Hokura, J.M. Kisler, S. Shogo, G.W. Stevens, Y. Komatsu, *Sep. Purif. Technol.* 48 (2006) 197–201.
- [47] H. Noh, S.T. Yohe, E.A. Vogler, *Biomaterials* 29 (2008) 2033–2048.